Proceedings of the IASS 2022 Symposium affiliated with APCS 2022 conference
Innovation·Sustainability·Legacy
19 – 22 September 2022, Beijing, China

A historical graphical analysis method for rigid frames

Shuyuan HAN*[a], Denis ZASTAVNI[a]

* Louvain research institute for Landscape, Architecture, Built environment [LAB]
Place du Levant 1 (L5.05.05) – B 1348 Louvain-la-Neuve
shuyuan.han@uclouvain.be

Abstract

This research reviews a historical graphical method for the analysis of rigid frames. As the basis of this method, the graphical analysis methods for statically indeterminate beams, as well as determinate ones, were also reviewed. This method for rigid frames was presented by William Wolfe in 1921 [1]. Although somewhat rudimentary and almost forgotten, it possesses a special cognitive value comparing to the analytical and numerical methods. The current mainstream of the study on graphic statics pays limited attention on the application of graphic statics to rigid frames, as well as to hyperstatic beams. However, exploration on the analysis methods of these structure types was an important part of the history of graphic statics. Such explorations have occupied a large portion of some of the classic works of graphic statics. After the introduction, this paper reviews the origin and basis of the graphical method for rigid frames, revealing the history and system of the technique behind the graphical method for rigid frames. The methods for beams will be explained in more technical details in the following section, enabling readers to readily comprehend the explanation of the method for rigid frames in the next part. After the technical account, the advantages and disadvantages of this method for rigid frames are discussed. The author argues that this graphical method for rigid frames, notwithstanding its present limitation, is potential to be developed into a design method for architects to explore the form of rigid frames perceptively.

Keywords: rigid frame, graphic statics, statical indeterminacy, bending moment diagram, elastic curve

1. Introduction

A Rigid frame is a load-bearing skeleton characterized by its continuous moment-resisting joints. The joints are so stiff comparing to members that the change of angles of joints under load are conveniently neglected generally. Due to the structural redundancy result from these rigid joints, rigid frames are often statically indeterminate, or termed as hyperstatic, which means that the inner forces cannot be calculated simply using the static equilibrium of forces and moment. The deformation of structures, and thus strengthen of material, must be involved as well.

Graphic statics is a geometric-based approach for the analysis and design of structures. The classic graphic statics is a powerful tool with unparalleled visual clarity, and it enjoyed worldwide popularity around the turn of the nineteenth and twentieth century. Nonetheless, its efficiency was limited by hand-drawing, one of the reasons leading to its declining popularity. It was almost totally superseded by algebraical and numerical methods by the end of the twentieth century in both teaching and practice. In recent years, graphics statics has been rediscovered as a perceptive method for structures design with an enhanced efficiency through computerization. During the “renaissance”, the graphic statics has been well studied, reintroduced, redeveloped for statical problems.

Though with “statics” in its name, the theories and techniques of graphic statics has well been extended further into the field of strength of material in history. Rigid frames, as well as hyperstatic beams, can be and has been analyzed with graphic statics. These theories and techniques comprise a substantial part of the arsenal of graphic statics. However, the methods for rigid frames, as well as for other statically indeterminate structures, have received much less attention. For example, the seminal book of E. Allen and W. Zalewski did not cover this topic at all [2]. The exceptionally comprehensive monograph on the history of structural theory by K. Kurrer highly valued graphic statics both for its historical significance and future promise, but only mentioned its application in hyperstatic structures in a passing comment [3]. The historical study of T. Boothby presented the graphical method for continuous span girders by Du Bois and Greene, and the long-forgotten graphical methods for portal frames by Milo Ketchum and Jerome Sondericker [4]. But the portal frame discussed are lattice, not rigid ones. E. Saliklis clearly explained and exemplified the techniques for statically indeterminate beams and determinate rigid frames [5], but still missed the ones for rigid frames; besides, the book is a textbook on know-how, shed little light on the history aspect. It is regrettable that a more complete review on the geometric-based methods for rigid frames and the highly-related methods for hyperstatic beams, is still missing. This fact is especially upsetting in light of the length that these topics occupied in many classic works of graphic statics. For example, in *Anwendungen der graphischen Statik* published by Ritter, a semi-graphical method for rigid frames was presented [6].

To this end, in the following section this paper will present an account on the history of the geometric-based method for rigid frames. More technique details will be explained in the next two sections. After that, there will be a discussion evaluating the advantage and drawbacks of the methods. The last part summarizes the main points and discusses the prospect of future research.

2. the origin and basis of the graphical method for rigid frames

This part presents a brief review of the graphical analysis methods for rigid frames from the historical perspective. As the foundation of this method, the graphical methods for funicular curves, beam bending moment, beam deflection, beam statical indeterminacy will be reviewed in turn.

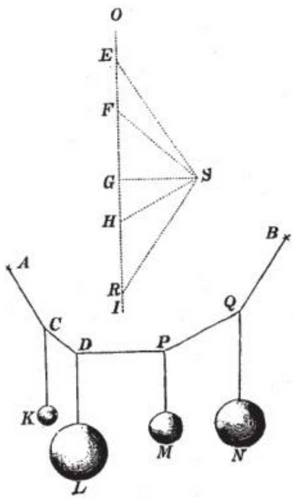

Figure 1 Force polygon (up) and funicular polygon (below) [8]

The foundation of the graphical analysis methods for rigid frames lies in Pierre Varignon's (1645-1722) introduction of the graphical method to determine the funicular polygon in his work *Nouvelle Mécanque ou statique* published posthumously in 1725 [7]. Varignon discovered that the funicular polygon, which is the resulting equilibrium position, and the tension of an inelastic suspended rope under loading could be determined with a fan-like polygon composed of a succession of triangles of forces, called force polygon. The funicular polygon is also termed as funicular curve or form diagram, while the force polygon as force diagram. For example, in figure 1 the edges of the funicular polygon of *ACDPQB* resulted from loads *K*, *L*, *M*, *N* can be constructed with the force polygon *SEFGHR*. The length of the vertical edge of each triangle represents the magnitude of each load, and the length of rays represents the magnitude of each segments of the funicular polygon, to which the rays are parallel one by one. Take the first triangle *EFS* for instance, the length of the vertical *EF* represents the weight of *K*. line *AC* and *CD* were drew in parallel to *ES*, *FS* respectively, with their intersection *C* on the vertical of load *K*. The remaining line segments of the two diagrams will also be drawn in the same manner.

The bending moment diagram of statically determinate plane beams simply supported at ends could be analogously constructed as a funicular polygon enclosed by a closing string joining the two ends of the funicular. This finding was made by Carl Culmann (1821-1881) in the first volume of his seminal book *Die graphische Statik* in 1864 [8]. The essence of Culmann's moment diagram was a graphical " integration machine", as historian Stüssi put it [9], contrasting the essence of the common moment diagrams: a simplified graph of the abscissa-moment function presenting calculation results. A more detailed explanation of Culmann's diagram can be found in the *section 3.1*.

In his book Culmann also showed a keen interest in statically indeterminate continuous beams over multiples spans, which were gaining widespread popularity in railway bridges then. However, Culmann did not manage to presented a graphical solution to this structural type. Because for the analysis of hyperstatic structure the consideration of deformation is indispensable, which he found too complicated to treat graphically. This inability is partly due to Culmann's equation of curvature was not simplified. He then entered into a somewhat abstruse analytical discussion of continuous girder [8].

It was Christian Otto Mohr (1935-1918) who was the first to graphically solve this problem, in his treatise *Beiträge zur Theorie der Holz- und Eisenkonstruktionen* (Contribution to the theory of wooden and iron constructions) published in 1868 [10]. There were two keys to his solution: the graphical method of deflection and the fixed-point method, which were both invented by him. First, with a simplified equation of curvature, Mohr deduced that the defection of beams could also be represented with funicular polygon. By analogically taking discretized moment as the 'loading', the deflection curve could be depicted by a funicular polygon with its closing string representing the original neutral axis of beam. Second, Mohr addressed the statical indeterminacy with the fixed-point method. This method is based on the fact that the abscissae of the inflexion point of unloaded spans is independent from its bending moment propagated from loaded spans. The fixed-point method for continuous beams was elaborated in-depth in the work of Augustus Jay Du Bois [11] and James B. Chalmers [12] and will not be detailed in this paper.

Also based on Culmann's moment diagram, the American engineer and theorist Charles Ezra Greene (1842–1903) presented a different semi-graphical approach for trussed hyperstatic continuous girders in his monograph in 1875 [13]. Greene's method combined moment-area theorem with the method of tentative closing string. The well-known moment-area theorem was first clearly presented in this book, despite partly implied in Mohr's above-mentioned treatise already. But Greene probably was not aware of Mohr's treatise then, as he had only acknowledged Culmann's work in this book. The procedure of Greene is to draw tentative closing string with trail end ordinates, then, with moment-area theorem calculate and check if relative deflection conforms. New closing strings will be tried until the correct one is located. Greene's method is well explained by Thomas Boothby [4], hence will not be explained in the following section.

Surely, it is also feasible to inspect the tentative closing string more graphically though Mohr's elastic curve instead of moment-area theorem. This hybrid approach was taken by William Sidney Wolfe, an American instructor and civil engineer, in his textbook *graphical analysis* published in 1921 [1]. Wolfe employed a graphical trick of locating the end of correct closing string based on trial ones, which, to the best of the author' knowledge, was first presented by him. Wolfe thus solved a number of different statically indeterminate beams, including continuous beams and ones with fixed ends, and, most interestingly, a rigid portal frame.

The highly-graphical solution for the portal frame is based on his solution for indeterminate beams. And to expound his method for indeterminate beams, explanation of techniques borrowed from the precursors mention above is inevitable. It is worth noting that rigid frames have also been solved graphically or semi-graphically with fixed-point method [7] [14].

3. The basic techniques of the graphical analysis methods for rigid frames

This part explains the technique basis of Wolfe's graphical analysis method for rigid frames. As abovementioned, the methods for rigid frames was based on the graphical methods for hyperstatic beams (*subsection 3.3*), which are in turn based upon the geometric-based method for simply supported beams (*subsections 3.1* and *3.2*). Most of the techniques in the *subsections 3.1* and *3.2* is well covered by Saliklis' book [5]. But since they are crucial to the topic in discuss, the author feels justified to cover the major points from a more historical perspective.

3.1. Culmann's geometric-based analysis of bending moment for statically determinate beams

To understand Culmann's bending moment diagram, we can start with the graphical solution of the moment of a force about a point. Take the case in figure 2 as an example, to calculate the moment of force *f* about the arbitrary point *K'*, a pair of reciprocal triangles are constructed. The first triangle △*OCD* is composed of line segment *DC*, drawn in parallels with *f* in any convenient scale, and segments joining endpoints *D*, *C* to an arbitrary pole *O*. To construct the second triangle △*O'C'D'*, from *O'*, an arbitrary point on the action line of *f*, draw line *O'C'* and *O'D'* parallel to *OC* and *OD* respectively. Point *C'* and *D'* are the intersections of these two lines with line *p*, the parallel line of *f* through *K'*. The distance between *f* and *C'D'* equals *h'*, while that between *O* and *DC* equals *h*. Because △OCD is obviously similar to △O'C'D', $CD \cdot h'$ *equals* $C'D' \cdot h$. It follows that:

$$M = |f| \cdot h' = CD \cdot h' = C'D' \cdot h \tag{1}$$

In which *M* is the moment of force *f* about *K'*.

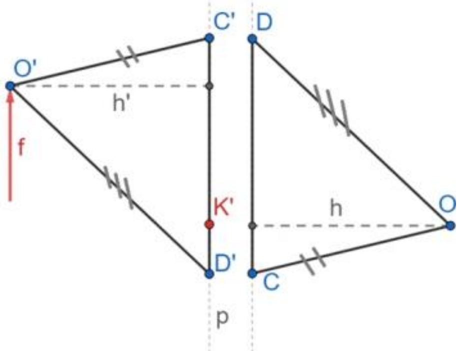

Figure 2 graphical solution of the moment of a force. Form diagram (above), force diagram (below) (source: author redrawn according to Wolfe 1921)

The bending moment diagram of a simply supported beam can be read as a succession of such reciprocal triangles. Take the simply supported beam under four loads in figure 3 for example. A funicular polygon *A'B'C'D'E'F'* is constructed with force polygon *ABCDEO* through Varignon's method, then the end points *A'* and *F'* are joined with a closing string, of which the parallel line though *O* intersects loading line *AB* on point *R*. The magnitude of the reaction force *5* under the left beam end must equal the length of line *AR* because it forms a closed triangle with *RO* and *AB*, which corresponds to the equilibrium on point *A'*. Similarly, the length of line *RE* equals to the reaction force *6* on the right end. The funicular polygon with its closing string is the bending moment diagram of the beam. To prove that, take the beam section on the arbitrary vertical *x* between load *3* and *4* for example. As $\triangle A'G'K'$ and $\triangle ORA$ are reciprocal triangles for reaction force *5,* according to the graphical solution of moment above, the moment of force *5* around any point of line *x* equals *G'K'* times the pole distance *h*. Similarly, moment of load *1* equals *J'K'* times *h*, that of load *2* equals *I'J'* times *h*, that of load *3* equals *H'I'* times *h*. As the moment direction of the load *1, 2, 3* are opposite to that of reaction *5*, the moment of the loads should be subtracted from that of the reaction *5* to obtain the resultant moment. Hence,

$$M_x = h{\cdot}G'K' - h{\cdot}J'K' - h{\cdot}I'J' - h{\cdot}H'I' = h{\cdot}G'H' \tag{2}$$

In which M_x is the resultant moment on vertical *x*.

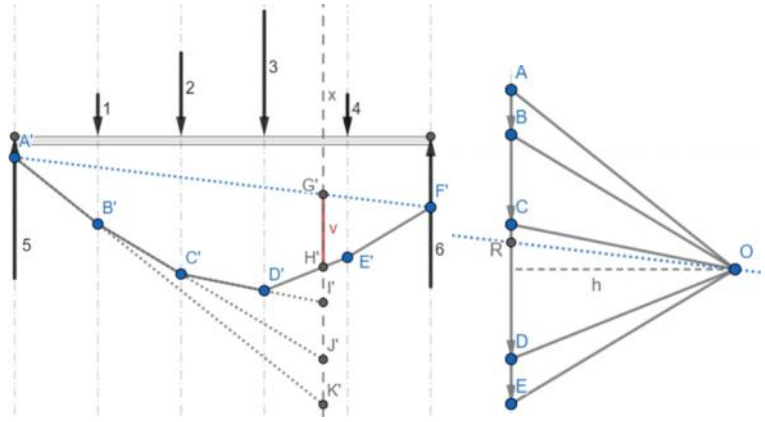

Figure 3 graphical solution of the moment of a force. Form diagram (left), force diagram (right) (source: author redrawn according to Wolfe 1921)

It follows that the moment at any section of a beam is given by the product of the pole distance times the its intercept. The intercept is the length of the segment cutting between the funicular polygon and its closing string. It is worth noting that the abscissa of pole O is in reverse proportion to the pole distance of force diagram, and the ordinate of pole affects the slope of the closing string but not the intercept for each section. As for beams subjected to continuously distributed load, the load should be discretized and integrated. In other words, the load should be evenly divided, and each division is substituted by an equivalent concentrated load imposed on the vertical of the centroid of the division. The final error will be marginal if the divisions are reasonably narrow.

3.2 Mohr's Geometric-based method for deflection analysis of statically determinate beams

Mohr's Geometric-based method for deflection can be readily understood if one understands the algebraically meaning of Culmann's moment diagram: integration machine". The construction process of Culmann's moment diagram is equivalent to double integrating the loading function. i.e.:

$$M(x) = \iint q(x)d^2x \tag{3}$$

Where *M(x)* is the function of bending moment along the abscissa *x*, *q(x)* the function of loading.

Since the function of deflection *w(x)* of a beam is also directly proportional to the double integration of the function of bending moment *M(x)*, i.e.:

$$w(x) = \frac{1}{EI}\iint M(x)d^2x \tag{4}$$

Where E is Young's modulus of material, I second moment of area about the neutral axis of the beam section. EI is bending stiffness, a value indicating the ability of the beam to resist bending.

It follows that the defection of a beam could also be computed through similar graphical device. By analogically taking moment as continuously distributed "load", the deflection function *w(x)* could be depicted by a funicular polygon with its closing string representing the original beam neutral axis. As the intercept between funicular polygon and closing string is reversely proportional to the pole distance of force diagram, the intercept will just equal deflection if the pole distance of its 'force diagram' is set as:

$$h = \frac{EI}{n \cdot H} \tag{5}$$

in which h is the pole distance of this special 'force diagram', n is a scale to scale down h in order to scale up the ordinate of elastic curves as deflection is normally tiny, H the pole distance of force diagram for constructing the bending moment diagram This special 'force diagram' for deflection was quite vaguely referred to as auxiliary figure (*Hülfsfigur*) by Mohr [10]. To differ from while be analogous to Culmann's conventional force polygon, this special 'force diagram' will be referred to as 'MΔx force polygon/diagram' following James Chalmers [12] or simply 'MΔx polygon/diagram'. Chalmers' writing is one of the earliest introductions of Mohr's method to English readers.

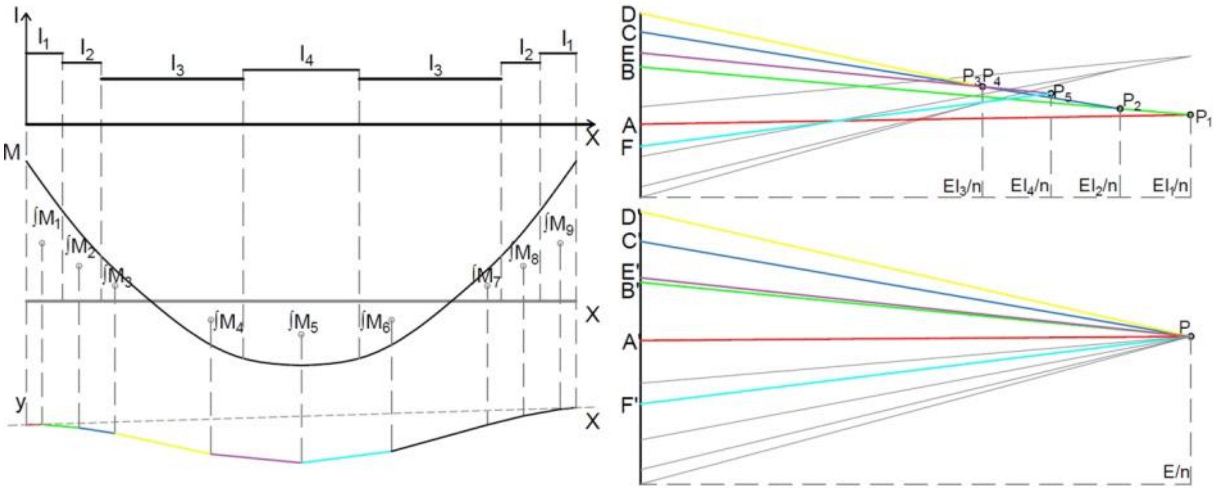

Figure 4 graphical solution of the elastic curve of a girder with given moment at ends. segments with the same color are parallel. The diagram of second moment of area of the girder (left above), given bending moment diagram (left middle), result elastic curve (left below), the MΔx polygon of the first method (right above), the MΔx polygon of the second method (right below) (source: author redrawn according to image from [10])

Mohr's method is advantageous when dealing with beams with varying second moment of area I. The girder with inconstant I under given moment in figure 4 is an example from Mohr's treatise. The bending moment is given. To accommodate to the inconstant second area moment and different signs of moment, Mohr divided the bending moment diagram into nine slices, within which the second area moment and the sign of moment are constant. On this basis, Mohr devised two alternative MΔx force polygons to accommodate inconstant second area moment. The first technique:

a) The magnitudes of areas of each discretized moment segment $\int M$ are treated as the "load". They are laid out in the order of the segment numbers vertically with the positive moment-area of segments *4, 5, 6* from top to bottom in turn and the negative moment-area of *1, 2, 3, 7, 8, 9* in the opposite direction.

b) The pole distance for each segment in proportional to its corresponding second area moment and equals $\frac{EI}{n \cdot H}$, in which I is the second moment of area about the neutral axis of the beam. Here, H is assumed to be one for convenience.

c) Each ray intersects the previous one or its extension on the pole.

For example, the third ray CP_2 intersects DP_3 at the pole P_3, while DP_3 intersects EP_4 at the pole P_4. P_3 and P_4 coincide as their pole distance both equals $E \cdot I_3/H$. The sixth ray FP_5 intersects the fifth ray EP_4 on its extension at the pole P_5 as the pole distance $E \cdot I_4/H$ is larger than that of P_4.

The second technique:

a) The magnitudes of moment-areas divided by respective second area moment $\frac{\int M}{I}$, are treated as the "loading". They are laid out in the order and direction as the first technique.

b) The pole distance h for each segment is fixed to equal $\frac{E}{n \cdot H}$, in which H is also assumed to be one.

c) Each ray intersects the previous one on the same pole.

The elastic curve is then constructed with parallels of each ray. Its vertices lie on the verticals drawn from the centroids of moment segments.

Essentially, the second MΔx force polygons a modification of the first MΔx force polygons scaling down every component triangle by the ration of its respective second area moment so that all the poles coincide. The MΔx force polygon looks simpler in the second methods, but the relation between second area moment and slope is less readable. It is worth noting that the direction of the first ray AP_1 or AP is arbitrary and the closing string representing the position of original neutral axis is not necessarily horizontal.

3.3. The techniques of Wolfe's geometric-based method for statically indeterminate beams

The problem of calculating the bending moment of statically indeterminate beams can resolves itself into locating the closing string, as shown in figure 5 the funicular curve of bending moment is solely dictated by loading. The influence from external moment and fixed ends is reflected by the location of closing string. for example, when there is a moment at support, the closing string detaches from the end of funicular curve in a vertical distance representing the magnitude of the moment at support.

It only takes two trials to locate the closing string of the moment diagram approximately by Mohr's trick of auxiliary paired triangles at ends. The beam fixed at both ends (figure 5) is an example from his book. After constructing the funicular polygon of moment, to determine the closing string, he started by drawing two closing strings *r-r'* and *s-s'* (in dashed lines) on this funicular polygon. He then constructed deflection lines m-m_1' and m-m_2', which is respectively corresponding to *r-r'* and *s-s'* with corresponding MΔx polygons. As both ends of the beam are fixed, the correct elastic curves should be tangent to the original neutral axis at ends. Therefore, *r-r'* and *s-s'* are wrong because the tangents to the ends of their corresponding elastic curves do not coincide with original neutral axes extended but make angles to them. The end of the correct closing string can be located based on the trial ones with a pair of similar triangles with opposite angles (enlarged view of the right end of closing string in figure 5). The right ends of both the right-end tangents and the neutral axes of the two trial elastic curves are extended rightward to the same arbitrary horizontal distance, making the vertical distances at the ends of W_1 and W_2. As W_1 is above the axe whereas W_2 below it, the real location of the right end of the closing string must lie somewhere between *R'* and *S'*. Measure off W_1 from R' on one side of R_2, then W_2 from S' on the other side. By connecting the extremes of these two lengths, the intersection X is obtained, which approximately locates the right end of the true base line. In a same way the left end Y is also be located. This is not a precise method, but Wolfe claimed that the error was marginal.

Note that his MΔx polygons is slightly different from Mohr's: all the "loads" of moment-areas were laid out on the loading line of in the same direction from up to bottom, and the poles of negative moment were set on the left side of the loading line.

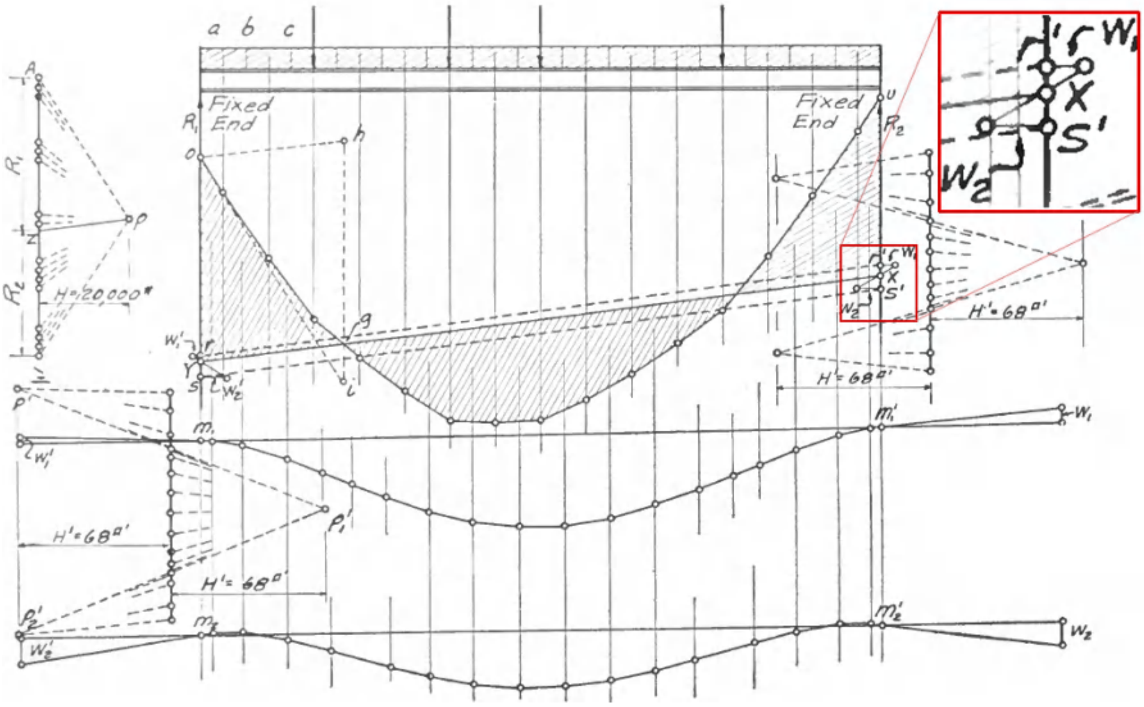

Figure 5 diagrams for a girder fixed at both ends. Force diagram (up left), loading and bending moment diagram (up middle) enlarged view of the right end of closing string(up right) , and MΔx polygon based on trial closing string RR' (middle right), the MΔx polygon based on trial closing string SS'(down left), elastic curves based on RR' and SS' (down middle) [1]

4. The techniques of Wolfe's graphical analysis method for rigid frames

This part presents the Wolfe's graphical analysis method of a steel portal frame. The frame has two fixed bases and a girder with varying second moment of area due to the stiffing plates on its webs (figure 6). The frame is loaded vertically by four point-loads and evenly distributed self-weight.

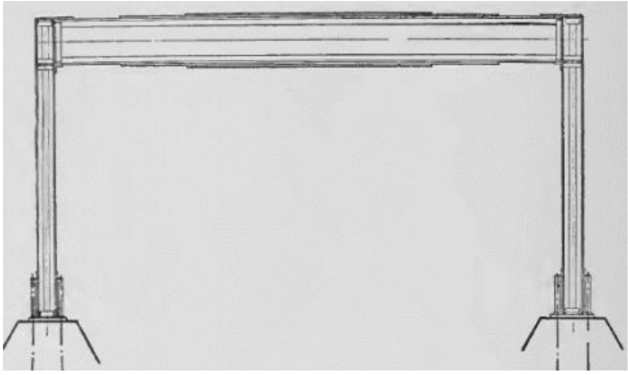

Figure 6. The portal frame that Wolfe analyzed with graphic statics [1].

Wolfe reduce the portal frame into a continuous beam over three spans. As shown in figure 7, the bending moment diagram of columns are revolved 90 degrees in opposite directions to horizontal around rigid joint *b* and *c*. The moment diagrams are then lowered altogether in order not to overlap the notation of loading and second area moment of the beam. Then, the rigid connections between beams and rotated columns are treated as continuous beam over simple support, because the displacement at the rigid joints between beam and columns is negligible, and moreover, the bending moment and the angle of rotation are continuous through the joint. The elastic curve will also be flattened in the same manner.

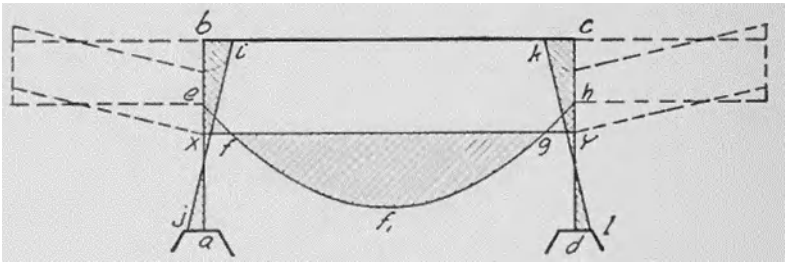

Figure 7. Transformation of the bending moment diagram [1]

The correct bending moment diagram could be determined based two tentative closing strings according to Wolfe. The funicular curve of the beam (the curve of *3* in figure 8), independent of moment at the beam ends, was first constructed from left to right according to the load with a force diagram (*2* in figure 8). Then with the first trial closing string (dotted line below in the moment diagram of beam), the first trial elastic curve (*5* in figure 8) is constructed accordingly with the auxiliary first trial M∆x diagram (*4* in figure 8). Note that the pole distance for the girder of the M∆x diagram varies according to second area moment. This elastic is evidently incorrect there is displacement blow both ends. Another trial elastic curve with displacement above both ends (*7* in figure 8) was constructed based on a different trial closing string (dotted line above in the moment diagram of beam). Then the correct closing string of moment was located with the auxiliary of a pair of similar triangles mentioned previously. It worth noting that, a simple analytical analysis was also employed by Mohr beforehand to determine the difference of the moment at the two ends of columns. thus, the moment closing strings of columns can be located in accordance with the ones of the beam.

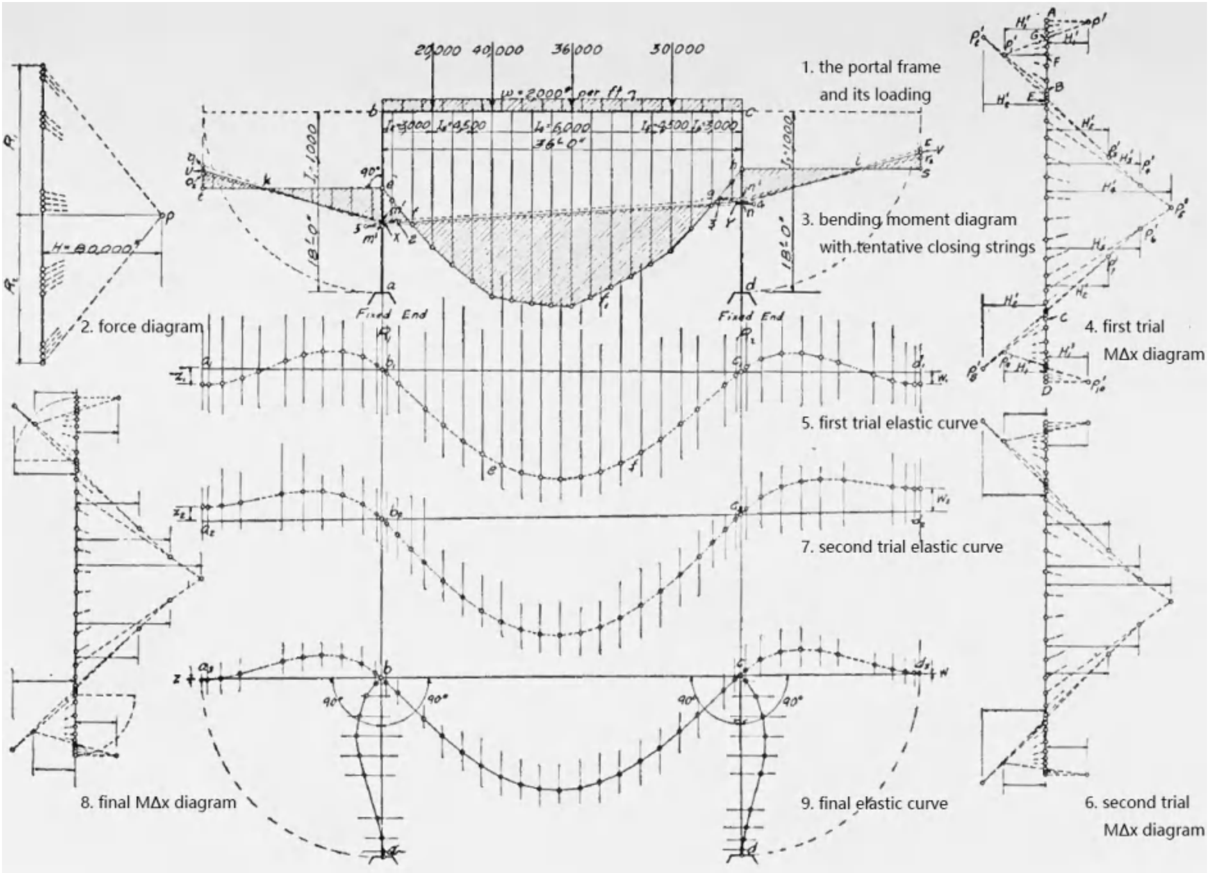

Figure 8. Diagrams for the portal frame including two tentative trials [1]

5. The values and drawbacks of the historical geometric-based method for rigid frames

The geometric-based method for rigid frames processes unique values compared with classic algebraic method. Firstly, the method can be advantageous for problems involving compound loading or varying moments of second area moment. Such problems can be difficult to formulate algebraically. Secondly, it can be easily grasped by ones without a good knowledge of calculus, which is the case for most architects. Thirdly, as the track of the entire analysis process and all the relations are clearly presented in the same set of drawing, it is possible to change both the geometry and its bending behavior and obtain a renewed equilibrium as long as related diagrams adapt accordingly. One can change the desired geometry and then understand how the bending behavior must adapt. Or, reversely, change the bending behavior and then obtain a geometry that adapts. It thus become a chronology-free because the deductive process undertaken by the designer can be switched whenever desired. Form and bending moment are simultaneously and dynamically steered by designers. Perhaps most importantly, this method is very insightful into the relation between form and forces. one can have a clearly idea of how loads affect bending, how beam’s bending stiffness affects deflection, instead of losing the sense of relations in the maze of calculation.

the first point eases the analysis of rigid frames with changing sections. The last three points, especially the last one, gives this method potential edge of aiding architects to study, perceive and design rigid frames. combined together, this method could leave a space for architect to explore the creative forms of rigid frames.

This method apparently has its drawback, which can partly account for to its current disuse. Firstly, the method can only be applied to symmetric frames under symmetric vertical loading. Moreover, this method has not been well developed for more complex frames, like multi-story and multi-span, frames with oblique or curved members. Its laborious hand-drawing aggravates this incompetence.

6. Conclusion and future work

This paper reviews a historical graphical analysis method for rigid frames with a brief historical overview and a technical explanation on this method and its supporting techniques. The special values and drawbacks of this historical geometric-based method is also discussed. In a whole, this paper gives a global perspective on this graphical method that has been long ignored, its merits and present limitation.

For future research, there are two possible approaches: history and design.

Wolfe's method is just one of the graphical methods for rigid frames. For a more comprehensive account on this topic, a historical study of the fixed-point method will be indispensable. Besides, the historical application in real design practices of Wolfe's method, as well as the fixed-point method, is to be investigated.

For the perspective of design, theoretical development and parameterization are still needed to overcome the limitation and achieve the potential of this method.

Acknowledgements

This research is funded by the China Scholarship Council (CSC), and its cofounding with UCLouvain.

References

[1] W. S. Wolfe, *Graphical analysis: a text book on graphic statics*. New York: McGraw-Hill, 1921.

[2] E. Allen and W**.** Zalewski, *Form and Forces: Designing Efficient, Expressive Structures*. New York: John Wiley & Sons, 2009.

[3] K. E. Kurrer, *The history of the theory of structures: searching for equilibrium.* (2nd ed.). John Wiley & Sons, 2018.

[4] T.E. Boothby, *Engineering Iron and Stone: Understanding Structural Analysis and Design Methods of the Late 19th Century.* American Society of Civil Engineers, 2015.

[5] E. Saliklis, *Structures: a Geometric Approach.* Springer, 2019.

[6] W. Ritter, *Anwendungen der graphischen Statik. Nach Professor C. Culmann. Dritter Teil: Der kontinuierliche Balken*. Zurich: A. Raustein, 1900.

[7] P. Varignon, *Nouvelle mecanique ou statique: dont le projet fut donné en MDCLXXXVII*. chez Claude Jombert, 1725.

[8] K. Culmann, *Die graphische statik. Volume 1*. Meyer & Zeller, 1864.

[9] F. Stüssi, "Karl Culmann und die graphische Statik." *Schweizerische Bauzeitung* 69.1 (1951): 1-3.

[10] C. Mohr, "Beiträge zur Theorie der Holz- und Eisenkonstruktionen", *Beiträge aus der Plasmaphysik*, vol. 14, pp. 20-52, 397-400, 1868.

[11] A. J. Du Bois, *The Elements of Graphical Statics and Their Application to Framed Structures: With Numerous Practical Examples of Cranes--bridge, Roof and Suspension Trusses.* John Wiley and son, 1877.

[12] J. B. Chalmers, *Graphical Determination of Forces in Engineering Structures*. Macmillan and Company, 1881.

[13] C. E. Greene, *Graphical Method for the Analysis of Bridge Trusses: Extended to Continuous Girders and Draw Spans*. D. Van Nostrand., 1875.

[14] E. Suter, *Berechnung des kontinuierlichen Balkens mit veränderlichem Trägheitsmoment auf elastisch drehbaren Pfeilern sowie Berechnung des mehrfachen Rahmens mit geradem Balken nach der Methode der Fixpunkte*. Springer-Verlag, 1916.